Delft University of Technology

Consistent approach to onset theory

Baar, Simon; Pavlov, Leonid; Kassapoglou, Christos

Important note
To cite this publication, please use the final published version (if applicable).
Please check the document version above.

Consistent approach to onset theory

Simon Baar[1] , Leonid Pavlov[2] and Christos Kassapoglou[3]

Abstract

Onset Theory (previously known as Strain Invariant Failure Theory) is a physics-based composite failure criterion attempting to predict failure at the level of constituents rather than for a homogenized ply. Applying Onset Theory correctly requires a number of steps. As a starting point for other researchers, a consistent approach is developed by resolving contradictions found in literature. This includes the micromechanical FEA process used to determine the individual fiber and matrix strains, such as correct choice of representative volume elements (RVEs), the use of transformed RVEs, boundary conditions, and the location of data extraction points. Analytical expressions are provided to determine the full state of strain in a ply, including in-plane and out-of-plane Poisson's strains and thermally induced mechanical strains. Literature definitions of the critical invariants are discussed, and a trend in critical distortional invariants is observed. Assumptions and limitations of the theory are identified. Finally, a failure envelope is compared to World Wide Failure Exercise test data.

Introduction

In 2001, Onset Theory was proposed in ref. 1 as Strain Invariant Failure Theory (SIFT). It attempts to predict failure at the constituent (fiber and matrix) level rather than for a homogenized ply. It was further developed in refs. 2, 3, and 4. Ref. 5 gives an overview of SIFT, including the choices made during development.

Many authors have published various versions of Onset Theory. This article provides a summarized, consistent approach to Onset Theory as a starting point for other researchers. Recently, ref. 6 had similar intent, but different focus. It is referenced where appropriate. This article provides additional insight, in particular how to determine the full state of strain (including thermally induced mechanical strains) analytically, and how to draw in-plane failure envelopes. Familiarity with the articles mentioned above is assumed, in particular regarding micromechanical enhancement (MME).

Onset Theory requires determining the homogenized state of strain of the laminate under combined loading (see *Homogenized State of Strain*), converting it to the dehomogenized constituent strains for each ply (see *Micromechanical Enhancement (MME)*), and calculating the first invariant and second deviatoric invariant of the strain tensor (see *Strain Invariants*). Failure is assumed to occur when any invariant reaches its critical value. The critical values are postulated to be independent of each other, the state of load, and the other constituent, i.e. there is no interaction between the invariants for fiber and matrix, and a given resin has the same critical invariants regardless of fiber material and applied loads. *Observations Regarding Distortional Invariants* lists some observations regarding the critical distortional invariants for various materials. *Summary of Consistent Approach* contains a list of all steps required to apply Onset Theory, while *Example Failure Envelope* provides a failure envelope based on World Wide Failure Exercise test data.

Micromechanical enhancement (MME)

During MME, unit strains are applied to representative volume elements (RVEs). Strain amplification factors are extracted from the FEA results. These are used to convert

[1]Odyssey Space Research, Houston, TX, USA
[2]Business Unit Manager CompositesLab, ATG Europe B.V., Noordwijk, Netherlands
[3]Delft University of Technology (TU Delft), Department of Aerospace Engineering, Delft, Netherlands

Corresponding author:
Christos Kassapoglou, Delft University of Technology, Department of Aerospace Engineering Rm 2.32, Kluyverweg 1, 2629 HS Delft, Netherlands.
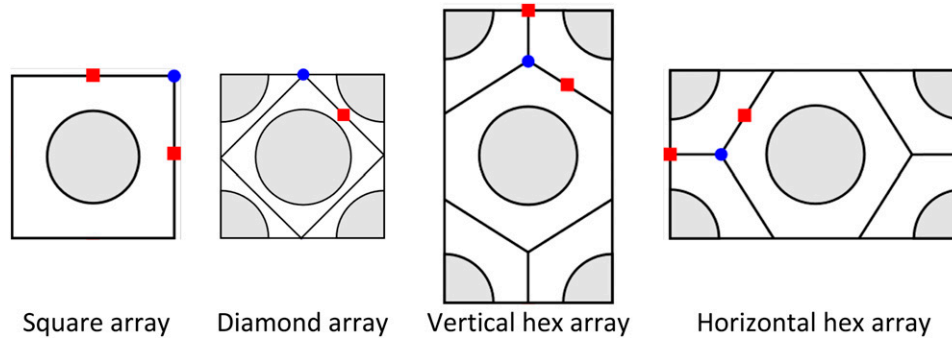Email: C.Kassapoglou@tudelft.nl

Figure 1. The four standard fiber arrays. Blue circles: interstitial location (where fibers are furthest apart). Red squares: interfiber location (where fibers are closest together).

the homogenized state of strain to dehomogenized constituent strains without requiring FEA for every new case. The state of strain is the vector of the six strain components. This raises three questions: which RVEs need to be analyzed (see *Fiber array types and transformed representative volume elements (RVEs)*), the boundary conditions (see *Boundary Conditions (BCs) on Representative Volume Elements (RVEs)*), and where to extract results (see *Interrogation Points*).

Fiber array types and transformed representative volume elements (RVEs)

One of the strongest claims regarding the types of RVEs is found in ref. 5: *"four standard fiber arrays can provide bounds on all of the possible random arrays [...]; the square array, the diamond array, and the two hexagonal arrays"*, *"two hexagonal arrays"* meaning horizontal and vertical long edges (see Figure 1). The authors of refs. 3 and 4 only mention square and hex fiber arrays, which is even more limiting. They also do not mention random arrays. Similarly, ref. 7 asserts that *"the square and hexagonal arrangements [...] have been shown to give bounding magnification factors and are assumed to exist somewhere in the random distribution of fibers in the laminate"*.

Contrary to that, a series of articles (in particular ref. 8) suggests using a square and a hex RVE, but transforming those RVEs by angles between 0° and 180°.

This article does not investigate whether regular fiber arrays are indeed accurate or conservative representations of a random fiber arrangement. It is only concerned with the necessary regular fiber arrays assuming that it is valid to use them in the first place. In regular fiber arrays, the fiber is assumed to be circular.

Limiting the investigation to regular RVEs, it can be shown that of the four proposed arrays (square, diamond, and vertical/horizontal hex) only a square and either one of

the two hex fiber arrays have to be analyzed using FEA. The results for the other two can be derived analytically. It is straightforward to verify that transforming the FEA results for a square array yields identical values to running FEA for a diamond array. This is discussed in detail in ref. 9. The underlying principle can be formalized as $M = \Theta^{-1} M' \Theta$, where M is the 6x6 matrix of mechanical strain amplification factors (relating the homogenized and dehomogenized strain vectors, see equation (16)) for an arbitrary angle, M' is the matrix for one of the two fundamental RVEs (square and hex), and Θ the applied transformation (using $c = \cos\theta$ and $s = \sin\theta$, where θ is the RVE angle):

$$\Theta = \begin{bmatrix} 1 & 0 & 0 & 0 & 0 & 0 \\ 0 & c^2 & s^2 & cs & 0 & 0 \\ 0 & s^2 & c^2 & -cs & 0 & 0 \\ 0 & -2cs & 2cs & c^2-s^2 & 0 & 0 \\ 0 & 0 & 0 & 0 & c & -s \\ 0 & 0 & 0 & 0 & s & c \end{bmatrix} \quad (1)$$

For the thermal amplification factors, a similar equation can be derived. Since they are a vector, only a single transformation $A = \Theta^{-1} A'$ is required. A and A' are the vectors of thermal amplification factors for the transformed and fundamental RVEs (relating the applied temperature difference to the dehomogenized constituent strain vector, see equation (16)).

Ref. 6 also concluded that the results of the square and hex RVEs can and should be transformed. They do not include the Θ^{-1} pre-multiplication for the mechanical amplification factors, which is acceptable in the context of Onset Theory because the properties of interest are invariants (and therefore coordinate system independent). The authors of the present article find it useful to include this transformation back to the original coordinate system to allow for numerical comparison of the resulting strain amplification factor matrices. Either way the validity of the approach can be confirmed vi-

sually in form of the failure envelopes (see the discussion of Figure 4).

The process to obtain M' and A' can be found in the standard literature on Onset Theory: the strain response for an applied unit strain ϵ_{11} determines the first column of M' and so on. A' is obtained from an applied unit temperature difference.

Results of a square cell transformed using $\theta = 45°$ are identical to FEA results of a diamond cell, though not for any single point (see discussion below). The same holds for vertical and horizontal hex arrays: one can be obtained from the other using the transformation with $\theta = 90°$, without running FEA.

In terms of the required angles, for the square cell angles of 0°, 90°, 180°, ... give identical results due to rotational symmetry. Since points in one half of the RVEs are used (see *Interrogation Points*), the same results are already obtained after 45°.

It should be emphasized that "the same results" is not intended to mean that any single point in the RVE returns the same results. The purpose of this application of Onset Theory is to draw failure envelopes. The proposed limited angle range causes the results of the two quadrants to be "switched". Since all points are used to determine the failure envelopes, the relative location is irrelevant.

Based on these symmetry considerations, the only required angles are therefore 0° to 45°. For the hex cell, the same reasoning shows that 0° to 30° are sufficient. Including interrogation points in one half of the RVE and using symmetry reduces the range from the one proposed by ref. 6 (0° to 180°).

In summary, for conservatism strain amplification factors based on angles between 0° and 45° for a square base cell, and between 0° and 30° for a hex base cell, are needed. The degree increments depend on the desired fidelity of the results.

Boundary conditions (BCs) on representative volume elements (RVEs)

To determine the strain amplification factors, three types of loads are applied: thermal, shear, and normal loads. For the normal load cases there is contradicting information. Given an applied load, say along the fiber, the remaining faces (on which primary load is not applied) can be forced to remain in place ("fixed BCs"), as chosen by one of the original authors of SIFT, Jon Gosse (see e.g. ref. 4). The other original author, John Hart-Smith, allows the remaining faces to freely, uniformly translate normal to their original position ("movable BCs"), see ref. 5. For thermal and shear load cases, all main sources (i.e. the ones mentioned in the *Introduction*) agree on using movable

BCs for thermal loads and allowing the faces of the RVE to warp under shear loads.

The correct BCs for the normal load cases can be determined by means of a thought experiment. Assume a RVE containing a single homogeneous isotropic material. In this case, dehomogenized and homogenized strains are the same. Clearly, this means amplification factors of 1 for mechanical loads. It turns out that this is equivalent to using fixed BCs. The enhancement factors are derived based on the application of a unit strain in one direction. If the faces are allowed to move, there will also be Poisson's contractions, which are also strains. These strains (which would also be measured by for example strain gauges) have to be included in the homogenized state of strain. In equation form, this can be expressed as follows, where the dehomogenized (subscript "d") strains are on the left, the matrix represents the amplification factors, and the homogenized (subscript "h") strains are on the right:

$$\begin{bmatrix} \epsilon_x \\ -v_{12}\epsilon_x \\ -v_{13}\epsilon_x \\ 0 \\ 0 \\ 0 \end{bmatrix}_d = \begin{bmatrix} 1 & 0 & 0 & 0 & 0 & 0 \\ 0 & 1 & 0 & 0 & 0 & 0 \\ 0 & 0 & 1 & 0 & 0 & 0 \\ 0 & 0 & 0 & 1 & 0 & 0 \\ 0 & 0 & 0 & 0 & 1 & 0 \\ 0 & 0 & 0 & 0 & 0 & 1 \end{bmatrix} \begin{bmatrix} \epsilon_x \\ -v_{12}\epsilon_x \\ -v_{13}\epsilon_x \\ 0 \\ 0 \\ 0 \end{bmatrix}_h \quad (2)$$

However, given an appropriate choice of homogenized state of strain, movable BCs are also correct. In that case, the homogenized state of strain should not contain Poisson's strains, because the Poisson's effect is already contained in the matrix of amplification factors:

$$\begin{bmatrix} \epsilon_x \\ -v_{12}\epsilon_x \\ -v_{13}\epsilon_x \\ 0 \\ 0 \\ 0 \end{bmatrix}_d = \begin{bmatrix} 1 & -v_{21} & -v_{31} & 0 & 0 & 0 \\ -v_{12} & 1 & -v_{32} & 0 & 0 & 0 \\ -v_{13} & -v_{23} & 1 & 0 & 0 & 0 \\ 0 & 0 & 0 & 1 & 0 & 0 \\ 0 & 0 & 0 & 0 & 1 & 0 \\ 0 & 0 & 0 & 0 & 0 & 1 \end{bmatrix} \begin{bmatrix} \epsilon_x \\ 0 \\ 0 \\ 0 \\ 0 \\ 0 \end{bmatrix}_h \quad (3)$$

Either formulation is correct, and the strain amplification factors can be converted from one to the other, as discussed in ref. 9. To use the correct applied strain, it is important to be aware of the choice of BCs used during FEA.

In many experiments (e.g. laminate tests), ϵ_x and ϵ_y are controlled. Similarly, FEA will return all six strain components. Movable BCs would require the additional step of removing all Poisson's effects. It is typically easier to use

fixed BCs and measure or calculate the full homogenized state of strain. This is discussed further in *Homogenized State of Strain*.

For thermal loads, a similar thought experiment confirms that movable BCS are correct. A temperature difference should not cause dehomogenized constituent strains which would cause failure. Since the material will expand or contract depending on the temperature, the strain-free state is achieved by allowing the boundaries to move. Ref. 6 arrived at the same conclusions and provides a complete summary of BCs. It should be strongly emphasized (as done in that article) that applied displacements in the long direction of the hex array need to be scaled by $\sqrt{3}$ in order to apply a unit strain.

Interrogation points

Since dehomogenized strains vary throughout the RVE, strain amplification factors have to be extracted at a number of "interrogation points". For the matrix phase, ref. 3 and all other articles involving Jon Gosse (who is one of the original developers of Onset Theory) state that the most critical ones are the interstitial (IS; where fibers are furthest apart) and interfiber (IF, where they are closest) locations. These are indicated in the fiber arrays in Figure 1. Ref. 6 additionally includes points at the fiber/matrix interface on radial lines passing from the center of the fiber through the interfiber and interstitial points.

Regarding the fiber, ref. 10 uses points at its center, as well as on the fiber boundary at 0°, 45° and 90° (as measured from the horizontal), for both the square and the hex

array. Others, e.g. ref. 11, use points at 0°, 30°, 60° and 90° on the fiber edge for the hex array.

Another aspect that should be considered is symmetry of the RVE. Ref. 3 only uses points in a single quadrant of the RVE, while ref. 11 uses points in one half of the RVE, and some authors such as ref. 12 investigate points around the entire fiber.

Ref. 9 investigated the necessary interrogation points based on the locations that were found to actually influence the failure envelope. Figure 2 shows an example of such an investigation. Distortional matrix failure envelopes based on a large number of interrogation points are drawn, and the points that contribute to the final failure envelope are indicated on schematics of the square and hex RVEs. A closer investigation of the contributions reveals that the points on the fiber/matrix interface have a minor contribution to the envelope and may only be critical due to the resolution of interrogation points or numerical inaccuracies when determining the intersection between failure envelopes.

Distortional fiber and dilatational matrix failure were analyzed the same way. It is important to note that the investigation was limited to a relatively small number of failure envelopes. To ensure capturing the most conservative behavior, a dense grid of interrogation points should be used (see Figure 3). Within the scope of that investigation only the interfiber points of the square and hex arrays proved to be relevant for distortional matrix failure, if minor contributions to the failure envelope attributed to numerical inaccuracies were excluded. However, since this was only a single investigation this should not be taken to mean that other points can be discarded. Points at 0° and 90° on the fiber boundary determined dilatational matrix failure. Interestingly, the commonly used interstitial location was never
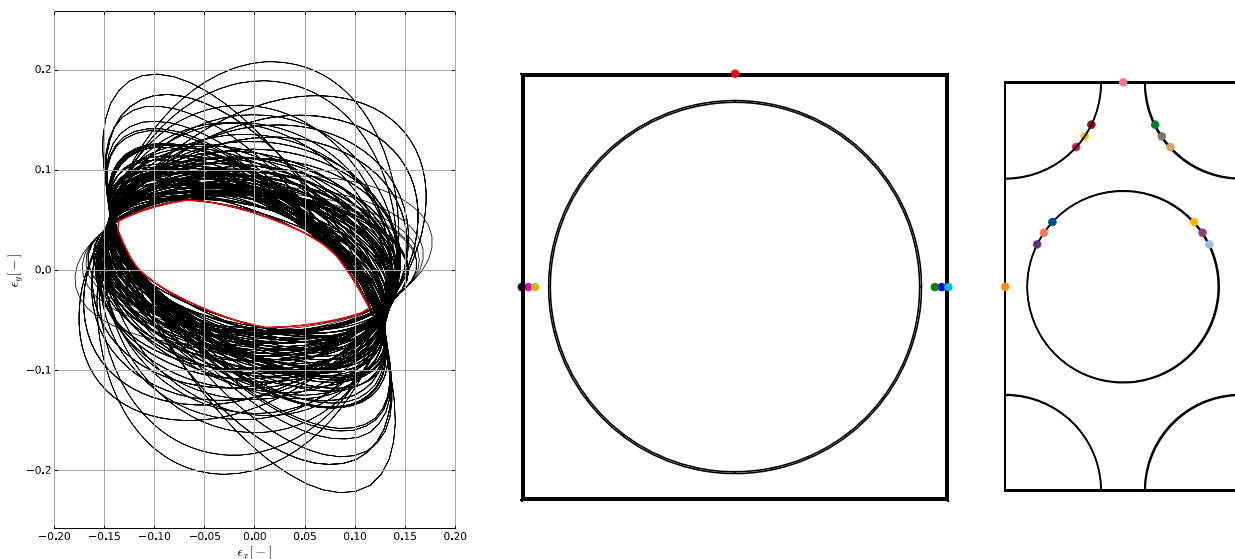

Figure 2. Location of critical interrogation points for distortional matrix failure envelope.
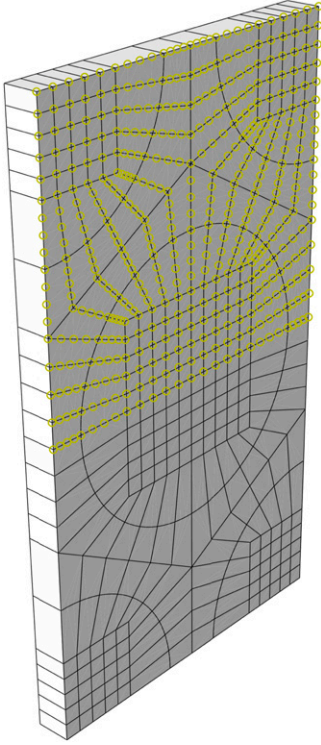
Figure 3. Example of dense grid of interrogation points (yellow circles) for a hex fiber array.
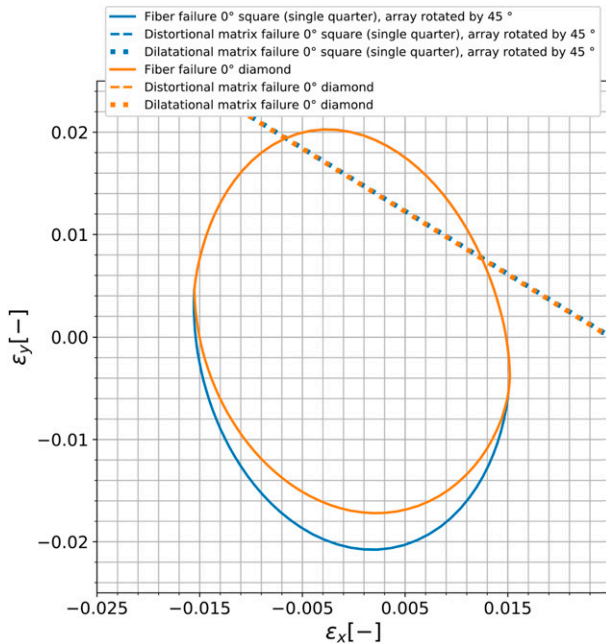

Figure 4. Necessity of using interrogation points in one half of the RVE.

critical for failure. For the fiber failure envelope, the fiber center and points at 0° and 90° on the fiber edge were critical.

In terms of symmetry, it can be shown that using interrogation points in a single quadrant is insufficient. Instead, interrogation points in one half of the RVE need to be used, as indicated in Figure 3. The reason is that for an applied shear strain, neighboring quadrants of the RVE will have normal strain response components of equal magnitude but opposite sign. This means that in the expression for the distortional strain invariant (see *Strain Invariants*), for terms such as $(\epsilon_{11} - \epsilon_{33})^2$ the value will be either added or subtracted, resulting in different failure predictions. It should be noted that this does not occur for the "standard" interrogation points for the matrix (interstitial and interfiber locations, as indicated in the fiber arrays in Figure 1). In these locations, FEA results do not show coupling terms (in other words, the normal strain response for an applied shear strain is zero).

Another argument is related to the transformation of RVEs, as discussed in *Fiber Array Types and Transformed Representative Volume Elements (RVEs)*. If a square array is transformed with interrogation points in a single quadrant only, it fails to reproduce the failure envelope produced by a diamond RVE. This is shown in Figure 4.

Using interrogation points in only a single quadrant of the square RVE is clearly unconservative in the compression regime compared to the diamond RVE. If interrogation points in one half of the square RVE are used, the transformed square RVE correctly recovers the diamond cell failure envelope. Note that, as discussed in *Fiber Array Types and Transformed Representative Volume Elements (RVEs)*, this does not mean that any individual point in the RVE returns the same results.

In summary, this means that it is insufficient to use interrogation points in a single quadrant of the RVE if it is transformed, or if interrogation points are used that cause a coupling between shear and normal strains. Therefore, it is necessary to use interrogation points in one half of the RVE.

Homogenized state of strain

The homogenized state of strain contains three contributions. First of all, there are strains due to mechanical loads. These should only be mechanical strains (not total strains, defined as $\frac{\Delta L}{L}$). This assumes that a homogeneous material does not fail under pure heating, which would create a total strain but no mechanical strains. In other words, to obtain the mechanical strains, the effect of free thermal contraction needs to be removed.

In addition to that, there are two types of strains that depend on temperature, both on the macro level and on the micro level. On the macro level, thermally induced mechanical strains due to the difference between the

application temperature and the curing temperature (assumed to be the strain free state) need to be taken into account. These occur due to a mismatch in thermal expansion coefficients of plies of different orientations. At the micro level, thermal strains arise due to the mismatch in thermal expansion coefficients of the constituents. These strains are determined using FEA and are included as the vector of thermal strain amplification factors, A.

As explained in *Boundary Conditions (BCs) on Representative Volume Elements (RVEs)*, if FEA was carried out for both the thermally induced mechanical strains and the applied strains, the results can be directly used as the homogenized state of strain. Else, the equations in *Poisson's Effects* and *Thermally Induced Mechanical Strains* can be used as a proposed approach to determine the missing strain components, e.g. in the typical case of having (ϵ_x, ϵ_y) failure data from tests. The proposed expressions have not yet been verified using full 3D FEA results, though this is in the plans for future work.

It should be emphasized that the expressions in this Section only capture applied in-plane strains. Similar equations could be derived for applied curvatures (i.e. bending).

Poisson's effects

Poisson's effects are an important aspect of the full state of strain. Neglecting it and using only the directly measured strains (e.g. ϵ_{11} and ϵ_{22} for the common case of in-plane normal strain envelopes) would be unconservative. The following derivation is based on classical lamination theory, which can be found in any standard textbook.

It is important to understand the use of ply and laminate properties. For the out-of-plane direction, the ply Poisson's ratio (in the ply coordinate system) should be used. This is due to the fact that in that direction the stress is assumed to be zero (plane stress conditions), meaning that each ply experiences a strain according to its own Poisson's ratios. On the other hand, for cases where in-plane Poisson's effects need to be taken into account (for example for failure envelopes involving only one of ϵ_x and ϵ_y, or for uniaxial tests with an unknown nonzero transverse strain), laminate properties (in the laminate coordinate system) should be used because of the assumption of in-plane strain compatibility made in classical lamination theory.

This means that in order to obtain the strain in a ply, a series of steps need to be followed. First of all, possible in-plane Poisson's effects have to be applied to the known laminate strains. Subsequently, the strains have to be transformed into the ply coordinate system. Finally, out-of-plane Poisson's effects need to be included. All of these steps are done in form of matrix multiplications. The resulting equation is $\epsilon_{applied} = \Pi_{out-of-plane} \, \Omega \Pi_{in-plane} \epsilon_{applied,laminate}$ where

$$\Omega = \begin{bmatrix} c^2 & s^2 & 0 & 0 & 0 & cs \\ s^2 & c^2 & 0 & 0 & 0 & -cs \\ 0 & 0 & 1 & 0 & 0 & 0 \\ 0 & 0 & 0 & c & -s & 0 \\ 0 & 0 & 0 & -s & c & 0 \\ -2cs & 2cs & 0 & 0 & 0 & c^2-s^2 \end{bmatrix} \quad (4)$$

($c = \cos\theta$ and $s = \sin\theta$, where θ is the angle between ply and laminate coordinate systems), and $\Pi_{out-of-plane}$ and $\Pi_{in-plane}$ are the appropriate choices of the matrices below. Measured ply properties in the ply coordinate system are used for the out-of-plane matrices, while laminate properties (derived using classical lamination theory) in the laminate coordinate system are used for the in-plane matrices. The terms used in the biaxial, out-of-plane matrix are terms of the stiffness matrix for an orthotropic material, such that $\sigma = C\epsilon$.

$$\Pi_{biaxial,out-of-plane} = \begin{bmatrix} 1 & 0 & 0 & 0 & 0 & 0 \\ 0 & 1 & 0 & 0 & 0 & 0 \\ -\dfrac{C_{13}}{C_{33}} & -\dfrac{C_{23}}{C_{33}} & 0 & 0 & 0 & 0 \\ 0 & 0 & 0 & 1 & 0 & 0 \\ 0 & 0 & 0 & 0 & 1 & 0 \\ 0 & 0 & 0 & 0 & 0 & 1 \end{bmatrix} \quad (5)$$

$$\Pi_{biaxial,in-plane} = \begin{bmatrix} 1 & 0 & 0 & 0 & 0 & 0 \\ 0 & 1 & 0 & 0 & 0 & 0 \\ 0 & 0 & 1 & 0 & 0 & 0 \\ 0 & 0 & 0 & 1 & 0 & 0 \\ 0 & 0 & 0 & 0 & 1 & 0 \\ 0 & 0 & 0 & 0 & 0 & 1 \end{bmatrix} \quad (6)$$

$$\Pi_{longitudinal,out-of-plane} = \begin{bmatrix} 1 & 0 & 0 & 0 & 0 & 0 \\ 0 & 1 & 0 & 0 & 0 & 0 \\ -v_{13} & 0 & 0 & 0 & 0 & 0 \\ 0 & 0 & 0 & 1 & 0 & 0 \\ 0 & 0 & 0 & 0 & 1 & 0 \\ 0 & 0 & 0 & 0 & 0 & 1 \end{bmatrix} \quad (7)$$

$$\Pi_{\epsilon_x,in-plane} = \begin{bmatrix} 1 & 0 & 0 & 0 & 0 & 0 \\ -v_{12} & 0 & 0 & 0 & 0 & 0 \\ 0 & 0 & 1 & 0 & 0 & 0 \\ 0 & 0 & 0 & 1 & 0 & 0 \\ 0 & 0 & 0 & 0 & 1 & 0 \\ 0 & 0 & 0 & 0 & 0 & 1 \end{bmatrix} \quad (8)$$

$$\boldsymbol{\Pi}_{transverse,out-of-plane} = \begin{bmatrix} 1 & 0 & 0 & 0 & 0 & 0 \\ 0 & 1 & 0 & 0 & 0 & 0 \\ 0 & -v_{23} & 0 & 0 & 0 & 0 \\ 0 & 0 & 0 & 1 & 0 & 0 \\ 0 & 0 & 0 & 0 & 1 & 0 \\ 0 & 0 & 0 & 0 & 0 & 1 \end{bmatrix} \quad (9)$$

$$\boldsymbol{\Pi}_{\epsilon_y,in-plane} = \begin{bmatrix} 0 & -v_{12}\dfrac{E_2}{E_1} & 0 & 0 & 0 & 0 \\ 0 & 1 & 0 & 0 & 0 & 0 \\ 0 & 0 & 1 & 0 & 0 & 0 \\ 0 & 0 & 0 & 1 & 0 & 0 \\ 0 & 0 & 0 & 0 & 1 & 0 \\ 0 & 0 & 0 & 0 & 0 & 1 \end{bmatrix} \quad (10)$$

It should be stressed that the out-of-plane matrix depends on the resulting state of strain in the ply co-ordinate system. This means that a 90° ply, loaded in uniaxial ϵ_x, should be using $\boldsymbol{\Pi}_{\epsilon_x,in-plane}$ for in-plane effects, but $\boldsymbol{\Pi}_{transverse,out-of-plane}$ for out-of-plane loads. For angles other than 0° or 90°, $\boldsymbol{\Pi}_{biaxial,out-of-plane}$ should be used. Each ply will be using a different Poisson's ratio matrix. The matrices above are a way of including the Poisson's strains on free edges. It is assumed that for purely uniaxial loads, the other edge is free to translate and the strain needs to be calculated using Poisson's effects, while for biaxial loads the strains on both edges are known.

Thermally induced mechanical strains

The thermally induced mechanical strains are based on the mismatch in thermal expansion coefficients between the ply and the laminate. The equations can once again easily be derived from classical lamination theory. By enforcing strain compatibility, the laminate thermal expansion coefficient can be calculated as

$$\boldsymbol{\alpha}_{laminate} = \begin{bmatrix} \alpha_{x,laminate} \\ \alpha_{y,laminate} \\ \alpha_{xy,laminate} \end{bmatrix} = \frac{\boldsymbol{Q}_{laminate}^{-1}}{t_{laminate}} \Sigma \boldsymbol{T}^T \boldsymbol{Q}_{ply} \boldsymbol{\alpha}_{ply} t_{ply} \quad (11)$$

For typical (i.e. symmetric balanced) laminates, the shear component should evaluate to $\alpha_{xy} = 0$. $\boldsymbol{Q}$ are the laminate or ply stiffness matrices, t refers to laminate or ply thickness as specified in the subscript, $\boldsymbol{T}$ is

$$\boldsymbol{T} = \begin{bmatrix} c^2 & s^2 & cs \\ s^2 & c^2 & -cs \\ -2cs & 2cs & c^2-s^2 \end{bmatrix} \quad (12)$$

and the ply material thermal expansion properties are $\boldsymbol{\alpha}_{ply} = \begin{bmatrix} \alpha_{x,ply} & \alpha_{y,ply} & 0 \end{bmatrix}^T$ (where the third component refers to shear, which – due to the orthogonality of a ply – is zero). Note that these coefficients are assumed to be constant with temperature.

Based on this, the in-plane thermally induced mechanical strains are calculated as the strains required to remove the discrepancy between the thermal expansion of the laminate and the free thermal expansion of a ply, in other words (in the ply coordinate system, and abbreviating thermally induced mechanical strains as ϵ_{TI})

$$\boldsymbol{\epsilon}_{TI,in-plane} = \begin{bmatrix} \epsilon_{x,TI,in-plane} \\ \epsilon_{y,TI,in-plane} \\ \epsilon_{xy,TI,in-plane} \end{bmatrix} = \left(\boldsymbol{T}\boldsymbol{\alpha}_{laminate} - \boldsymbol{\alpha}_{ply} \right) \varDelta T \quad (13)$$

As discussed previously, these strains cause additional Poisson's effects. Therefore, the final equation is

$$\boldsymbol{\epsilon}_{TI} = \boldsymbol{\Pi}_{biaxial,out\ of\ plane} \begin{bmatrix} \epsilon_{x,TI,in-plane} \\ \epsilon_{y,TI,in-plane} \\ 0 \\ 0 \\ 0 \\ \epsilon_{xy,TI,in-plane} \end{bmatrix} \quad (14)$$

It should be emphasized that these strains are very important for matrix failure. They have the same effect as applied external strains. As an example, in Figure 7 dilatational matrix failure at $\epsilon_y = 0$ is predicted in the 90° ply at $\epsilon_x = 0.007$, spot on with the suspected matrix cracking observed in test. This prediction includes thermally induced mechanical strains of $\epsilon_{x,curing} = 0.0038$. In other words, the dilatational matrix capability is reduced from 10,800 microstrain to 7000 microstrain, a reduction of about 35%.

Strain invariants

Two strain invariants are used in Onset Theory. The first is the dilatational strain invariant, given by $J_1 = \epsilon_{11} + \epsilon_{22} + \epsilon_{33}$. ϵ_{11}, ϵ_{22} and ϵ_{33} are components of any strain tensor using an orthogonal basis (see any of the sources listed in the *Introduction*). This is a reduced version; the full expression for the dilatational strain invariant is $J_1 + J_2 + J_3 = (\epsilon_{11} + 1)(\epsilon_{22} + 1)(\epsilon_{33} + 1) - 1$. Since J_2 and J_3 are related to the square and cube of strains, they are negligible for small strains.

For the distortional strain invariant, several versions are used in literature, all related to each other through a direct algebraic operation. The most common version is to use the equivalent strain (also known as von Mises strain due to its resemblance to the well-known von Mises yield criterion for isotropic materials), see equation (15).

$$\epsilon_{eqv} = \sqrt{\frac{1}{2}\left[(\epsilon_{11} - \epsilon_{22})^2 + (\epsilon_{11} - \epsilon_{33})^2 + (\epsilon_{22} - \epsilon_{33})^2\right] + \frac{3}{4}\left[\gamma_{23}^2 + \gamma_{13}^2 + \gamma_{12}^2\right]} \tag{15}$$

Note that this equation is using engineering shear strains, e.g $\gamma_{23} = 2\epsilon_{23}$. This is also why a factor $\frac{3}{4}$ appears in front of the shear terms, instead of a factor 3.

The relationship between the equivalent strain and the second deviatoric strain invariant (J_2'), as well as other common versions used in literature, is shown in Table 1.

These different definitions can cause confusion or even incorrect results when looking at numerical values. In fact, if these varying definitions are taken into account, some trends in the critical invariants can be observed, as discussed next.

Observations regarding distortional invariants

An extensive literature study of critical distortional invariants showed that the critical invariants for carbon fibers and E-glass are all similar, approximately $\epsilon_{eqv}^{*f} = 0.02 \pm 10\%$. As shown in Figure 5, 9 of 16 entries in Table 2 fall in this range, 3 more in $\pm 15\%$, and the other 3 (the biggest outliers) are all from a single source.

Thermoset resins show the same behavior, with $\epsilon_{eqv}^{*m} = 0.2 \pm 10\%$. The analysis is more involved since several values are suspected to be using a different definition of the critical distortional invariant than stated in the source. Table 3 and Figure 6 show the results. Where applicable, the suspected definition is used. If the suspicions are correct,

only 8 of the 30 critical invariants are >10% off, and only 4 more than 12%.

The cause is unclear, but to the knowledge of the authors this has not been published before. Composites using fibers from IM7 or AS4 to E-glass have vastly different strengths, so the similarity in critical strain invariants must be due to stiffness effects. Either the same homogenized failure strain results in different failure strengths, or due to MME identical dehomogenized constituent strains correspond to different homogenized strains. The former would be related to differences in the stiffness of the composite, while the latter would mean the individual constituent stiffnesses (together with e.g. fiber volume fraction) are the relevant factor. Ref. 9 contains a more thorough critical review of the sources.

Summary of consistent approach

This section is intended as a step-by-step procedure to apply Onset Theory.

Assumptions and limitations

Onset Theory in general, and the MME process in particular, is highly idealized. It assumes that RVEs are acceptable to obtain dehomogenized constituent from macro level strains. This implies that the lamina consists of a single, infinitely repeating type of RVE. Fibers are assumed to be perfectly circular. *Fiber Array Types and Transformed Representative Volume Elements (RVEs)* discussed these assumptions. Additionally, the analyses assume temperature-invariant material properties.

Onset Theory is a ply failure criterion (i.e. it is not used to predict interply failures such as delaminations). It works on

Table 1. Comparison of distortional invariant definitions.

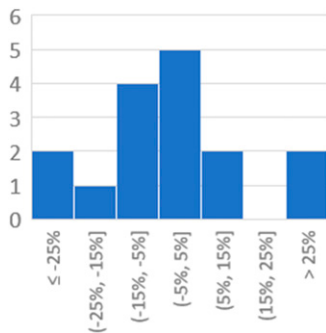| Definition	#1 (e.g. ref. 5)	#2 (e.g. ref. 2)	#3	#4 (e.g. ref. 13)
Expression	$\epsilon_{eqv} = \sqrt{3J_2'}$	$\frac{1}{\sqrt{3}}\epsilon_{eqv} = \sqrt{J_2'}$	$\epsilon_{eqv}^2 = 3J_2'$	$\frac{1}{3}\epsilon_{eqv}^2 = J_2'$

Figure 5. Distribution of ϵ_{eqv}^{*f} around 0.02.
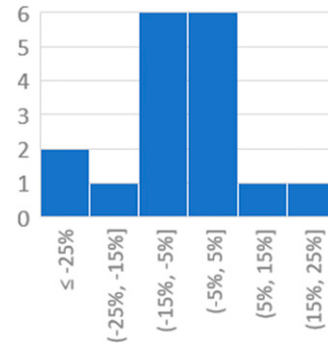

Figure 6. Distribution of ϵ_{eqv}^{*m} around 0.2.

Table 2. Critical distortional fiber invariants.

Source	Material combination	ϵ_{eqv}^{*f}	Deviation from $\epsilon_{eqv}^{*f} = 0.02$
Ref. 14, Table 8.4	T300/BSL914C	0.0133	−34%
Ref. 15, Table 3	T700/CU200NS	0.01495	−25%
Ref. 16, Table 3	CCF300/5228	0.017	−15%
Ref. 16, Table 3	CCF300/5428	0.018	−10%
Ref. 5 and others citing Jon Gosse	IM7/977–3	0.0182	−9%
Ref. 17, Table 5-11	E-glass/MTM57	0.0189	−6%
Ref. 14, Table 8.4	AS4/3501–6	0.019	−5%
Ref. 10, Table 1	IM7/K3B	0.0195	−3%
Ref. 18, Table 1	E-glass/MY750	0.0194	−3%
Ref. 19, Section 4.2	IM7/977–3	0.02	0%
Ref. 20, Table 5	IM7/5250–4	0.0204	2%
Ref. 21, Table 4	AS4/3501–6	0.021	5%
Ref. 22, Table 6-3	E-glass/RTM6	0.022434	12%
Ref. 16, Table 3	T700/5428	0.023	15%
Ref. 14, Table 8.4	E-glass 21xK43/LY556	0.0266	33%
Ref. 14, Table 8.4	E-glass 1200tex/MY750	0.0349	75%

Table 3. Critical distortional matrix invariants.

Source	Material combination	Critical invariant and definition (stated/suspected)	ϵ_{eqv}^{*m} (Based on suspected definition)	Deviation from $\epsilon_{eqv}^{*m} = 0.2$
Ref. 16, Table 3	CCF300/5228	0.144 (#1)	0.144	−28%
Ref. 17, Table 5-11	E-glass/MTM57	0.1472 (#1)	0.1472	−26%
Ref. 20, Table 5	IM7/5250–4	0.16 (#1)	0.16	−20%
Ref. 5 and others citing Jon Gosse	IM7/977–3	0.103 (#1/#2)	0.178	−11%
Ref. 10, Table 1	IM7/977–3	0.179 (#1)	0.179	−11%
Ref. 1, Table 3	T300/5208	0.0339; 0.0331 (#1/#3)	0.184; 0.182	−8%; −9%
Ref. 18, Table 1	E-glass/MY750	0.036; 0.0313 (#1/#3)	0.190; 0.177	−5%; −12%
Ref. 13, Section 4.1	T800s/3900–2	0.03434 (#4/#3)	0.185	−7%
Ref. 19, Section 4.2	IM7/977–3	0.11 (??/#2)	0.191	−5%
Ref. 16, Table 3	CCF300/5428	0.195 (#1)	0.195	−3%
Ref. 2, Tables 1 and 2	Carbon/glassy polymer	0.1144; 0.1124; 0.1164; 0.114 (#2)	0.198; 0.195; 0.202; 0.197	−1%; −3%; 1%; −1%
Ref. 21, Table 4	AS4/3501–6	0.198 (#1)	0.198	−1%
Ref. 16, Table 3	T700/5428	0.202 (#1)	0.202	1%
Ref. 23 Tables 4 and 5, Ref. 24 Table 2, Ref. 25 Section 3, Ref. 26 Table 5-3	T800s/3900–2	0.119; 0.117; 0.118; 0.113 (#2)	0.206; 0.203; 0.204; 0.196	3%; 1%; 2%; −2%
Ref. 23 Tables 4 and 5, Ref. 26 Table 5-2, Ref. 27 Table 4	T300/Cycom 970	0.1125; 0.1186; 0.1184; 0.118; 0.121; 0.122 (#2)	0.195; 0.205; 0.205; 0.204; 0.210; 0.211	−3%; 3%; 3%; 2%; 5%; 6%
Ref. 15, Table 3	T700/CU200NS	0.04919 (#1/#3)	0.222	11%
Ref. 22, Table 6-3	E-glass/RTM6	0.020069 (#1/#4)	0.245	23%

thin, flat, orthotropic plies and laminates under plane stress. The equations in *Homogenized State of Strain* do not include bending loads, although analytical expressions for these cases can be derived as well.

Physically, Onset Theory asserts that there are two independent failure modes for any material: distortion and dilatation, and that carbon fibers only fail in distortion. Dilatational fiber failure would be another non-interactive cutoff on the failure envelope. However, there are no critical dilatational fiber invariants in literature.

Onset Theory does not include (micro)structural failures such as fiber kinking. Adding these types of failure modes as additional non-interactive cutoffs on the failure envelope should be a high priority research item.

It should be emphasized that Onset Theory should not be modified to use stress instead of strain invariants. Unlike

stress invariants, strain invariants are independent of each other. There is an influence of the hydrostatic component of the stress (but not strain) on yield. This is not captured by the von Mises yield criterion. There are several other reasons, including a strain rate dependency of the critical stress (but not of the critical strain), as well as different failure stresses (but not strains) in compression versus tension. Ref. 26 explains these reasons in detail.

Micromechanical enhancement (MME)

It is important to use a consistent order of strain components during MME. In this article, the order will be $\begin{bmatrix} \epsilon_{11} & \epsilon_{22} & \epsilon_{33} & \gamma_{23} & \gamma_{13} & \gamma_{12} \end{bmatrix}^T$.

Amplification factors should be extracted from a dense grid of interrogation points in one half of the RVE (see *Interrogation Points*). As discussed in *Fiber Array Types and Transformed Representative Volume Elements (RVEs)*, square and hex fiber arrays are sufficient, transformed by 0° to 45° (square) and 0° to 30° (hex cells).

As *Boundary Conditions (BCs) on Representative Volume Elements (RVEs)* mentioned, ref. 6 came to the same conclusions about displacements and BCs for the RVE. These results will not be repeated here. The strain response at the interrogation points is used to determine $\boldsymbol{M'}$ and $\boldsymbol{A'}$ (see *Fiber Array Types and Transformed Representative Volume Elements (RVEs)*).

The mechanical amplification factors for ϵ_{22} for the hex cell need to be multiplied by $\sqrt{3}$ to scale to an applied unit strain for that direction. Alternatively, the BC could be written as $v = y_1$ at y_1, i.e. $v = 1$ at y_1 for the square cell and $v = \sqrt{3}$ at y_1 for the hex cell. This is done for shear, where the size of the RVE is included in the BCs.

Evaluating failure

Using the expressions in *Strain Invariants*, failure occurs if either of the two invariants exceeds its critical value, i.e. $J_1 > J_1^*$ (for the dilatational strain invariant) or $\epsilon_{eqv} > \epsilon_{eqv}^*$ (using the equivalent strain as the distortional strain invariant – any of the definitions in *Strain Invariants* can be used to determine distortional failure). The asterisk indicates the critical value. As emphasized in *Strain Invariants*, the same definition of the invariant has to be used for actual and critical distortional strain invariants.

The available literature agrees that for typical carbon fibers, dilatational failure does not occur, while for resins both types of failure are observed. For example, according to ref. 5, "Carbon fibers used in the aerospace industry today fail by distortion, regardless of the nature of the load. They do not fail by dilatation".

The strains in these equations are the components of the dehomogenized state of strain, given by
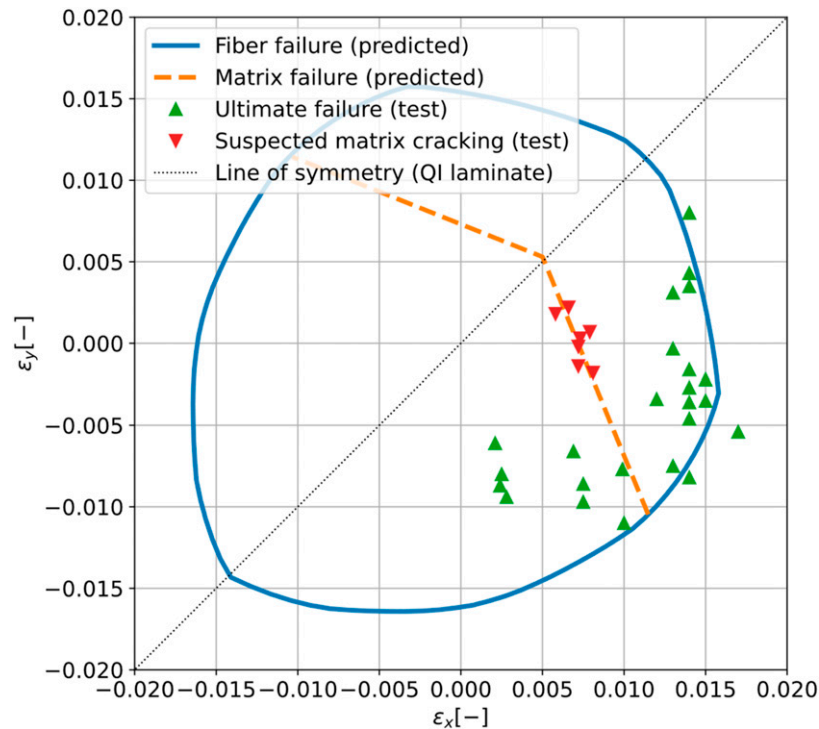

Figure 7. Comparison between prediction and biaxial strain test data for an AS4/3501−6 [90/±45/0]s laminate.

$$\boldsymbol{\epsilon}_{dehomogenized} = \boldsymbol{M}\boldsymbol{\epsilon}_{homogenized} + \boldsymbol{A}\Delta T \qquad (16)$$

where ΔT is the applied temperature difference, and $\boldsymbol{M}$ and $\boldsymbol{A}$ were derived in *Fiber Array Types and Transformed Representative Volume Elements (RVEs)*. Every combination of the two unique fiber arrays (hex and square), RVE transformation angles, and interrogation points should be investigated.

$\boldsymbol{\epsilon}_{homogenized}$ is given by $\boldsymbol{\epsilon}_{homogenized} = \boldsymbol{\epsilon}_{applied} + \boldsymbol{\epsilon}_{curing}$. As discussed in *Homogenized State of Strain*, these strains can be obtained from FEA or analytical expressions. Note that the expressions in this article were derived for applied in-plane rather than bending strains.

Example failure envelope

Using the consistent approach, failure envelopes were generated for several cases, including the AS4/3501-6 bi-axial failure envelope from the WWFE (ref. 28). Constituent and lamina material properties can be found in Table 1-3 of that article. The curing temperature (assumed to be the strain free state) as well as the ultimate failure strains are available in Table 2 of refs. 29 and 30, while the location of suspected matrix cracking is reported in ref. 31. Finally, the "default" critical invariants from *Strain Invariants* are used.

Figure 7 shows the resulting failure envelope. Matrix cracking is predicted very closely, while the ultimate failure predictions were less accurate. In particular for compression-dominated states of strain, predictions were unconservative. A likely cause is that Onset Theory does not include microstructural failure modes such as fiber kinking. These failure modes should be added in form of other (non-interactive) cutoffs of the failure envelope in strain space.

The other point to note is the large scatter of the test data in the compression-dominated regime. On the same radial line, i.e. for the same strain ratio, values between $\epsilon_y = -0.0061$ and $\epsilon_y = -0.0094$ are obtained, a difference of almost 55%. This makes comparing predictions and test data challenging.

Finally, a perfect failure criterion, using the exact material properties from the test specimen, should predict the result achieved by a perfect test. In reality, some tests may even overachieve the perfect test results due to scatter in material properties. However, typically factors decreasing the test result such as manufacturing flaws will be more prevalent. This may be a partial explanation for the trend in the tension-dominated regime, where the failure predictions form an outer bound on the test data, with very few data points outside of the predicted envelope.

Conclusions

This paper summarizes recent findings which provide researchers with a consistent starting point for using Onset Theory.

One major open question which is outside the scope of this work is whether or not regular fiber arrays are a physically meaningful, accurate, or at the very least conservative, representation of the true random fiber array. Following the consensus in previously published literature on Onset Theory (see *Fiber Array Types and Transformed Representative Volume Elements (RVEs)*) the discussion in this paper is limited to regular fiber arrays. In that case, it was found that square and hex fiber arrays should be analyzed, and additional arrays should be included by transforming the results between 0° and 45° (square) and 0° and 30° (hex). The faces of the RVE should be fixed in place during mechanical analysis but allowed to move during thermal analysis. Finally, data should be extracted from a dense grid of points in one half of the RVE, including points on the fiber/matrix boundary.

Analytical expressions for the full state of strain of a ply are developed, including Poisson's strains and contributions from thermally induced mechanical strains. Alternatively, an FEA model could be used to determine these strains.

Critical distortional invariants (in this paper expressed as equivalent strain) are surprisingly consistent across materials and material classes: for most carbon and glass fibers $\epsilon_{eqv}^{*f} = 0.02 \pm 10\%$, and for most resins $\epsilon_{eqv}^{*m} = 0.2 \pm 10\%$. At present the causes are unknown.

Applying the approach to test data obtained from the World Wide Failure Exercise shows excellent predictions of matrix cracking and good agreement for ultimate failure in tension/tension and tension/compression where tension is dominating. Tension/compression failure where compression is dominating is poorly predicted, which may be due to failure modes not included in Onset Theory (e.g. fiber kinking).

ORCID iD

Simon Baar ⓘ https://orcid.org/0000-0002-4764-6373

References

1. Gosse JH and Christensen S. Strain invariant failure criteria for polymers in composite materials. In: *42nd AIAA/ASME/ASCE/AHS/ASC Structures, Structural Dynamics, and Materials Conference and Exhibit*. Anaheim, CA, 2001. DOI: 10.2514/6.2001-1184

2. Pipes RB and Gosse JH. An onset theory for irreversible deformation in composite materials. In: *17th International Conference on Composite Materials (ICCM-17)*, http://www.iccm-central.org/Proceedings/ICCM17proceedings/Themes/Behaviour/ANALYSISFORFLIGHTCERT/F2.3ByronPipes.pdf (2009).

3. Buchanan DL, Gosse JH, Wollschlager JA, et al. Micromechanical enhancement of the macroscopic strain state for advanced composite materials. *Compos Sci Technol* 2009; 69: 1974–1978.

4. Ritchey AJ, Dustin JS, Gosse JH, et al. Self-Consistent Micromechanical Enhancement of Continuous Fiber Composites. In: Attaf B (ed) *Advances in Composite Materials - Ecodesign and Analysis*. InTech, pp. 607–624.

5. Hart-Smith LJ. Application of the strain invariant failure theory (SIFT) to metals and fiber-polymer composites. *Philos Mag* 2010; 90: 4263–4331.

6. Pearce GMK, Mukkavilli A, Chowdhury NT, et al. Strain Invariant Failure Theory – Part 1: an extensible framework for predicting the mechanical performance of fibre reinforced polymer composites. *Compos Struct* 2019; 209: 1022–1034.

7. Tran TD, Kelly DW, Prusty BG, et al. Micromechanical modelling of test specimens for onset of dilatational damage of polymer matrix in composite materials. In: *18th International Conference on Composite Materials (ICCM-18)*. 2011.

8. Ha SK, Jin KK and Huang Y. Micro-mechanics of failure (MMF) for continuous fiber reinforced composites. *J Compos Mater* 2008; 42: 1873–1895.

9. Baar S. *Onset theory (strain invariant failure theory): consistent approach and automation*. Delft University of Technology, http://resolver.tudelft.nl/uuid:a9ef5fcc-9f00-4b99-9625-7e3acbc92996 (2017).

10. Yudhanto A, Tay T-E and Tan. Micromechanical characterization parameters for a new failure criterion for composite structures. *Key Eng Mater* 2006; 306–308: 781–786.

11. Li X, Guan Z, Li Z, et al. A new stress-based multi-scale failure criterion of composites and its validation in open hole tension tests. *Chin J Aeronaut* 2014; 27: 1430–1441.

12. Tay T-E, Tan VBC and Liu G. A new integrated micro-macro approach to damage and fracture of composites. *Mater Sci Eng B Solid-state Mater Adv Technol* 2006; 132: 138–142.

13. Lee D and Yoshioka K. Distortional deformation of matrix in open-hole tension composites: experimental investigation. In: *20th International Conference on Composite Materials (ICCM-20)*. Copenhagen, 2015.

14. Wang CH. Progressive multi-scale modeling of composite laminates. In: *Multi-Scale Modelling of Composite Material Systems*. Woodhead Publishing, pp. 259–277.

15. Kim M, Park S, Park J, et al. Micro-mechanical Failure prediction and verification for fiber reinforced composite materials by multi-scale modeling method. *J Korean Soc Aeronaut Sp Sci* 2013; 41: 17–24.

16. Li Z, Guan Z, He W, et al. Strain invariant failure theory invariant properties of domestic carbon fiber/resin composites. *Acta Mater Compos Sin* 2011; 28: 192–196.

17. Mao Y. *Micromechanical modelling for failure of fibre reinforced composite materials*. The University of New South Wales, 2011.

18. Holmberg JA, Lundmark P and Mattsson D. Micromechanical vs lamina based failure theories. In: *13th European Conference on Composite Materials (ECCM-13)*. Stockholm, Sweden, 2008.

19. Tsai HC and Elmore J. SIFT Analysis of TiGr Laminates. In: *35th International SAMPE Technical Conference*. Dayton, OH, 2003.

20. Ng SJ, Felsecker A and Meilunas R. SIFT Analysis of IM7/5250-4 Composites. In: *36th International SAMPE Technical Conference*. San Diego, CA, 2004.

21. Lu S Compressive damage simulation of carbon fiber reinforced polymer matrix composite laminate open-hole structures based on strain invariant failure theory. *Acta Mater Compos Sin* 2015; 32: 1573–1580.

22. McNaught S. *Implementation of the strain invariant failure theory for failure of composite materials*. The University of New South Wales, 2009.

23. Tran TD, Kelly DW, Prusty BG, et al. A micromechanical sub-modelling technique for implementing Onset Theory. *Compos Struct* 2013; 103: 1–8.

24. Tran TD, Simkins D, Lim SH, et al. Application of a scalar strain-based damage onset theory to the failure of a complex composite specimen. In: *28th International Congress of the Aeronautical Sciences*, http://www.icas.org/ICAS_ARCHIVE/ICAS2012/PAPERS/923.PDF (2012).

25. Lim SH, Pearce GM, Kelly DW, et al. New developments in onset theory for onset of resin failure in fibre reinforced composites. In: *19th International Conference on Composite materials (ICCM-19)*. Montreal, Canada, 2013.

26. Tran TD. *Development of micromechanical modelling procedures using the Onset theory for failure of composites*. University of New South Wales, 2012.

27. Tran TD, Kelly DW, Prusty BG, et al. Micromechanical modelling for onset of distortional matrix damage of fiber reinforced composite materials. *Compos Struct* 2012; 94: 745–757.

28. Soden PD, Hinton MJ and Kaddour AS. Lamina properties, lay-up configurations and loading conditions for a range of fibre-reinforced composite laminates. *Compos Sci Technol* 1998; 58: 1011–1022.

29. Swanson SR and Christoforou AP. Response of quasi-isotropic carbon/epoxy laminates to biaxial stress. *J Compos Mater* 1986; 20: 457–471.

30. Swanson SR and Nelson M. Failure properties of carbon/epoxy laminates under tension-compression biaxial stress. In: Kawata K, Umekawa S and Kobayashi A (eds) *Composites '86: Recent Advances in Japan and the United States*. Tokyo: Proceedings of the Third Japan-US Conference on Composite Materials, 1986, pp. 279–286.

31. Soden PD, Hinton MJ and Kaddour AS. Biaxial test results for strength and deformation of a range of E-glass and carbon fibre reinforced composite laminates: failure exercise benchmark data. *Compos Sci Technol* 2002; 62: 1489–1514.